Jurnal Teknologi

Full Paper

EFFECT OF HEAT TREATMENT ON THE CHARACTERISTICS OF ELECTROLESS ACTIVATED CARBON-NICKEL OXIDE NANOCOMPOSITES

Adekunle Moshood Abioye[a,b], Soheila Faraji[a], Farid Nasir Ani[a*]

[a]Faculty of Mechanical Engineering, Universiti Teknologi Malaysia, 81310 UTM Johor Bahru, Johor, Malaysia
[b]Department of Mechanical & Production Engineering, Abubakar Tafawa Balewa University, Bauchi, Bauchi State, Nigeria

Article history
Received
25 January 2017
Received in revised form
15 April 2017
Accepted
25 May 2017

*Corresponding author
farid@mail.fkm.utm.my

Graphical abstract

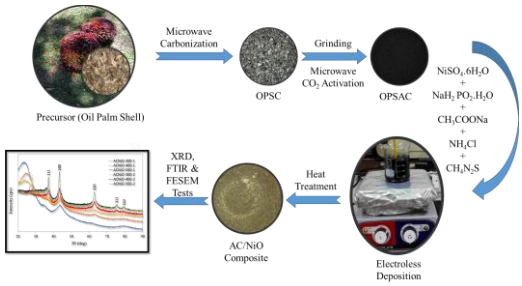

Abstract

Over the years, different experimental techniques have been employed to prepared activated carbon-metal oxide composite materials. However, some of these methods entail cutting-edge equipment and long processing time which may result in the destruction of the carbon structure. Electroless plating, which is a simple and efficient method, have been used to deposit nickel oxide nanoparticles on activated carbon prepared from oil palm shell (OPS) using microwave –assisted CO_2 activation. The nanocomposites have been heated at various temperatures (300, 400 and 500 °C) for 1 and 2 h. The prepared activated carbon has BET surface area and total pore volume of 574.37 m^2 g^{-1} and 0.244 cm^3 g^{-1}, respectively. The optimum heat treatment temperature has been found to be 400 °C. Also, the weight percent composition of nickel has been shown to increase with increase in treatment time.

Keywords: Nanocomposite, electroless plating, nickel oxide, microwave activation, activated carbon

1.0 INTRODUCTION

Currently, extensive research on nickel oxide/carbon (NiO/C) nanocomposites have been on the increase due to their applications' prospect in a variety of areas such as adsorption and purification purposes [1], production of fuel cells [2], hydrogen storage purposes [3] and manufacture of sensors [4] and electrodes [5]. Many experimental techniques such as microwave assisted heating [6], wet impregnation [7], electrodeposition [8], magnetron sputtering [9], thermal evaporation [7] and co-precipitation [10] have been used to prepare carbon-metal composites. However, some of these methods entail cutting-edge equipment and extended processing periods which may result in the destruction of the carbon structure. Although, wet impregnation is the most widely used among these methods, however, it lacks good control of the morphology and particle size [3]. Conversely, electroless plating is an efficient route to deposit metal nanocomposite and produce a uniform coating with unique properties on a wide variety of substrates [11, 12].

Electroless plating as a coating technique was developed by Abner Brenner and Grace E. Riddell of the National Bureau of Standards in 1946, and the first patent was assigned to them in 1950 [13, 14]. Electroless plating is an autocatalytic process

involving the chemical reduction of aqueous metal ions coated to a base substrate without the passage of external current. Electroless deposition is a coating technique whereby the selective reduction of the metal ions take place only at the surface of a catalytic substrate dipped in an aqueous solution of the said metal ions [13]. The metal ions reduction in the solution and the film deposition is accomplished by the oxidation of the reducing agent present in the solution. From available literature, nickel deposition by hypophosphite may be represented by the following equations:

$$Ni^{+2} + H_2PO_2^- + H_2O \rightarrow Ni^0 + H_2PO_3^- + 2H^+ \quad (1)$$

$$H_2PO_2^- + H_2O \rightarrow H_2PO_3^- + H_2 \quad (2)$$

Overall

$$Ni^{+2} + 2H_2PO_2^- + 2H_2O \rightarrow Ni^0 + 2H_2PO_3^- + 2H^+ + H_2 \quad (3)$$

The structure, morphology, thickness and hardness of electroless nickel deposit are significantly affected by the deposition time and heat treatment [15]. Though there are reported studies on the effect of plating time and heat treatment on the corrosion behavior of electroless Ni-P coating [15, 16], however, there is no literature on the effect of heat treatment on the characteristics of oil palm shell based-activated carbon-nickel oxide composites, to the best of our knowledge. Therefore, this study aimed at investigating how the characteristics of the AC-NiO nanocomposites prepared by electroless plating are affected by the heat treatment of the composites.

2.0 METHODOLOGY

2.1 Preparation of Activated Carbon

A two-step microwave-induced physical (CO_2) activation was implemented for the production of activated carbon from oil palm shell (OPS). Carbonization of OPS took place in a microwave (1 kW, 2.45 GHz) at a temperature of 800 °C at a heating rate of 50 °C min^{-1} under N_2 flow rate of 1 L min^{-1} for 20 min. The resultant char was activated at a temperature of 900 °C in a microwave at a heating rate of 50 °C min^{-1} under CO_2 flow rate of 400 cm^3 min^{-1} for 40 min. The AC was cooled down to room temperature under N_2 flow rate of 1 L min^{-1}. The as-prepared AC was put in a sealed bottle and kept in a desiccator for further analysis.

2.2 Preparation of AC-NiO Nanocomposites

Activated carbon-nickel oxide (AC-NiO) nanocomposites were fabricated by electroless deposition of Ni on active carbon in an electroless nickel solution. All the reagents used were of analytical grade (AR grade). Sigma-Aldrich supplied all the reagents and were used as supplied devoid of any purification. The AC particles were dispersed in distilled water with ultrasonic cleaner (WiseClean) at 45 °C for 30 min prior to the electroless nickel plating. The AC particles were immersed in aqueous baths with the composition and deposition conditions as presented in Table 1. The amount of AC used for the deposition was kept constant (1 g) [17]. The deposition time was kept at 1 h at the temperature specified in Table 1.

Table 1 Composition and deposition condition of the Electroless bath

Compound	Chemical composition	Content (g L^{-1})
Precursor	Nickel (II) sulfate ($NiSO_4.6H_2O$)	30
Reducing agent	Sodium hypophosphite ($NaH_2PO_2.H_2O$)	30
Complexing agent	Sodium acetate (CH_3COONa)	35
Buffer	Ammonium chloride (NH_4Cl)	25
Stabilizing agent	Thiourea (CH_4N_2S)	0.002
pH	8 – 9	
Temperature	80 – 90 °C	
pH adjuster	Sodium hydroxide (NaOH)	As required

After plating, the samples were filtered and dried in the furnace at a temperature of 300, 400 and 500 °C at a heating rate of 15°C/min and held for 1 and 2 h to obtain AC-NiO samples. After cooling down, the samples were put in bottles and labeled ACNiO-300-1, ACNiO-400-1, ACNiO-500-1 and ACNiO-300-2, ACNiO-400-2 and ACNiO-500-2, respectively.

2.3 Physiochemical Characterizations

The porosity of the AC was studied by conducting N_2 adsorption-desorption isotherm measurements at -196 °C using a surface area porosimeter system (Micromeritics 3Flex 3.01). The surface organic structures of the composite samples were investigated using Fourier Transform Spectrophotometer with PerkinElmer instrument. The composition and surface morphology of the composites were studied by energy dispersive spectroscopy (EDS) (Oxford INCA 400) and field-emission scanning electron microscopy (FESEM, HITACHI SU8020), respectively. The X-ray diffraction (XRD) patterns of the composites were performed using Rigaku diffractometer (SmartLab Thin Film) employing Cu Kβ radiation at 40 kV, 30 mA.

3.0 RESULTS AND DISCUSSION

3.1 Pore Structure Characterization of the AC

The N_2 adsorption-desorption isotherm of the as-prepared AC is depicted in Figure 1, showing that the as-prepared AC is microporous material, evidenced by the Type I isotherm. The characteristics of the as-prepared AC is shown in Table 2. According to the data in the table, the microporous nature of the AC is further confirmed with micropore volume accounting for 81% of the total pore volume.

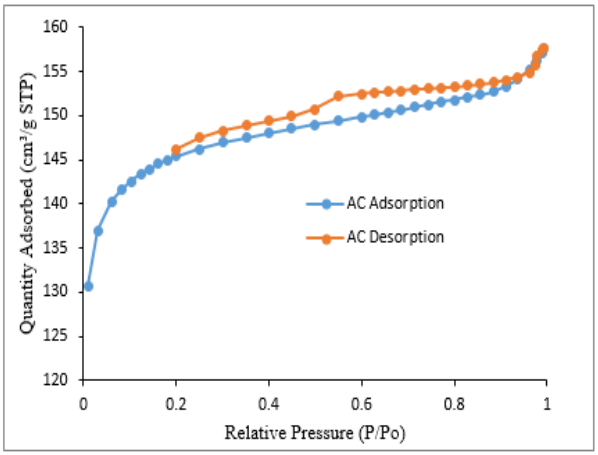

Figure 1 N_2 adsorption-desorption isotherm of the AC

Table 2 Characteristics of the AC

Subject		Activated carbon
BET surface area	(m^2 g^{-1})	574.37
Total pore volume	(cm^3 g^{-1})	0.244
Micropore volume	(%)	81.15
Mesopore volume	(%)	18.85
Average pore diameter	(Å)	16.96

3.2 Surface Chemistry Characterization Studies of AC-NiO nanocomposites

The FTIR spectroscopy is a versatile technique used to monitor changes in the surface functional groups of the composite materials. Figure 2 shows the FTIR spectra of AC-NiO composite samples. As shown in the figure, the FTIR spectra of the samples calcinated for 1 h show similar absorption bonds but with varying degree of intensity. The same thing goes for the samples calcinated for 2 h. A broad peak around 3436 cm^{-1} was observed in all the samples treated for 1 h. The absorption peak at 3436 cm^{-1} is ascribed to O–H stretching vibration mode of the hydroxyl functional group. The relative intensity of the peak at 3436 cm^{-1} was lower in the samples treated for 2 h. The presence of a peak at 3742 cm^{-1}, in the samples treated for 2 h, is ascribed to free O–H group. In samples treated for 1 h, the C–H stretching peaks at 2920 and 2856 cm^{-1} indicate the reduction of –COOH groups on the surface of activated carbon [18], whereas in samples treated for 2 h the band is shifted to 3016 cm^{-1} with high intensity. In the region of 1400-1700 cm^{-1}, two peaks located at 1632 and 1401 cm^{-1} could be observed in the spectra of the samples calcinated for 1 h, whereas in the samples calcinated for 2 h, the spectra show additional one peak located at 1692 cm-1. The peaks around 1560 cm^{-1} are related to the carboxylate anion stretch mode [19]. The peaks around 1077 cm^{-1} are attributed to oxygen functional groups such as C–O stretching of the carboxylic group [20]. In the FTIR spectra of the ACNiO-500-1, ACNiO-400-2 and ACNiO-500-2, two major peaks located at 470 and 568 cm^{-1} are observed in the region of 600-400 cm^{-1}, whereas only one peak located at 568 cm^{-1} is observed in the ACNiO-300-1, ACNiO-400-1 and ACNiO-400-2 FTIR spectra. The absorption bonds at 470 and 568 cm^{-1} can be ascribed to the Ni–O stretching vibration, thus confirming the formation of pure NiO nanoparticles.

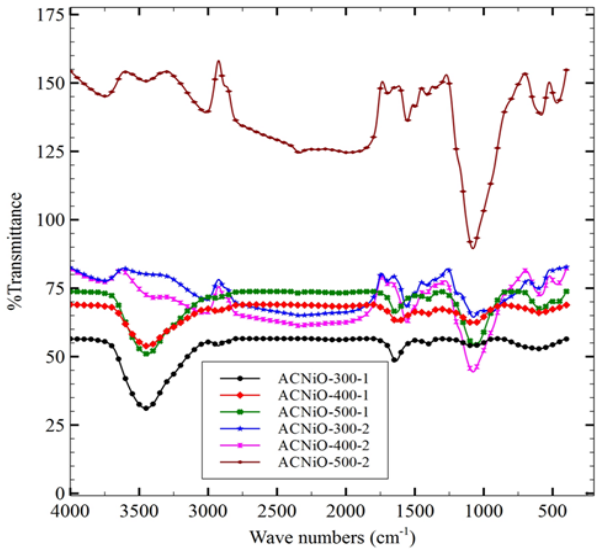

Figure 2 FTIR spectra of AC-NiO nanocomposite samples calcinated at 300, 400 and 500 °C for 1 and 2 h

3.3 Microstructure of AC-NiO Nanocomposites

Figure 3 depicts the FESEM images of the electroless AC-NiO composites with various heat treatment "temperature and time". It is clearly observed that the morphology is flake-like with porous open channels within the flake morphology. A close observation of the FESEM images indicates that flaky morphology grows rapidly with increment in the heat treatment temperature, similar to observation by Jahromi *et al*. [21]. The corresponding EDS spectra are shown in Figure 4. The peaks of Ni observed in the

EDS data confirmed the existence of Ni in the nanocomposites.

The EDS spectra show the elemental composition of the nanocomposites revealing the presence of nickel and traces of phosphorous which comes from the sodium hypophosphite used as reducing agent in the electroless nickel solution. The amounts of Ni, C, O and P elements on the surface of the nanocomposite samples by mass fraction are presented in Table 3. From the table, samples ACNiO-400-1 and ACNiO-400-2 have higher Ni mass fraction among the samples treated for 1 h and 2 h, respectively. These results are in agreement with the largely recognized optimal heat treatment regime of 400 °C [22]. Furthermore, Table 3 illustrates that the Ni mass fraction increases with increasing in calcination time.

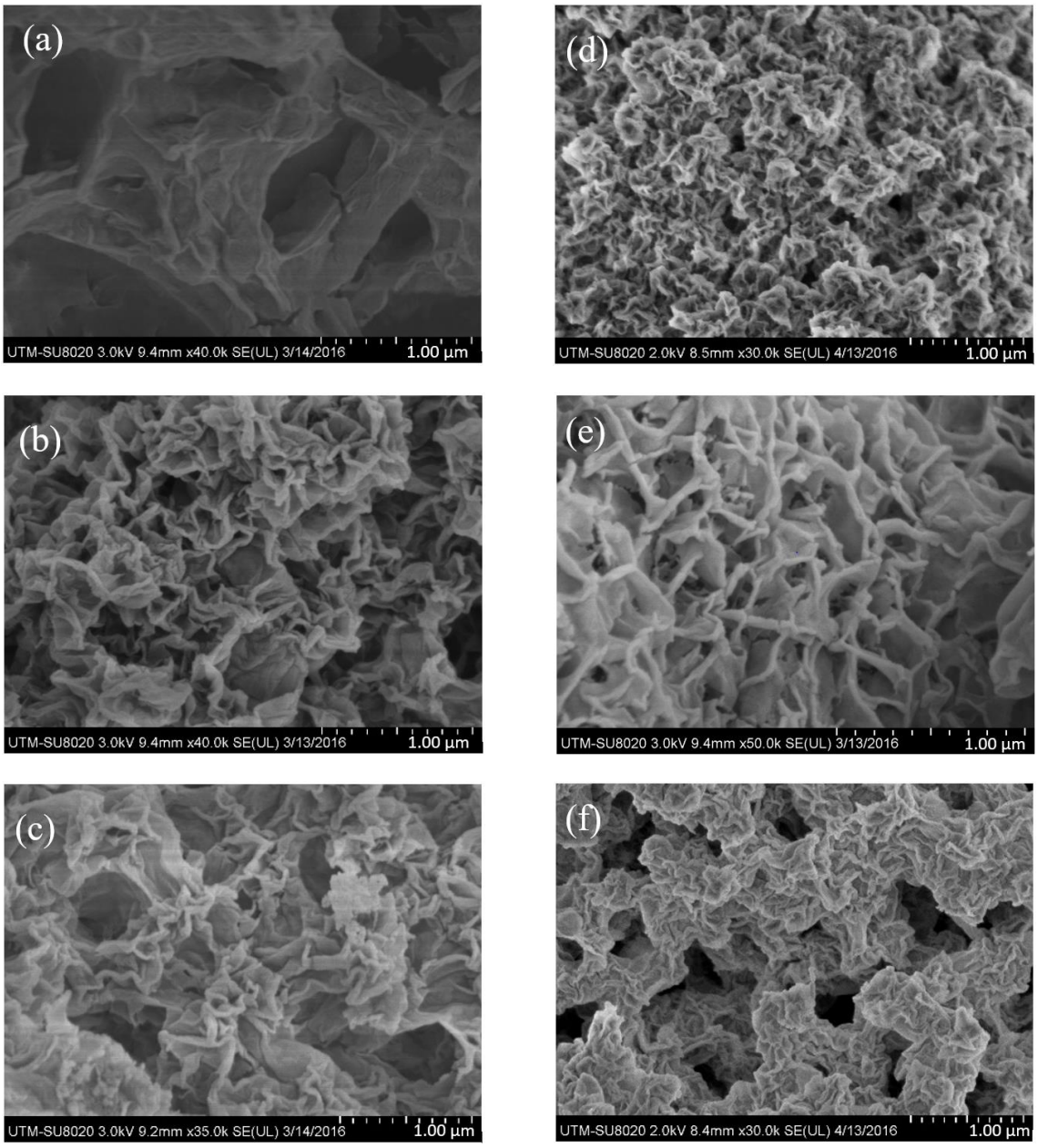

Figure 3 FESEM image for the (a) ACNiO-300-1, (b) ACNiO-400-1, (c) ACNiO-500-1, (d) ACNiO-300-2, (e) ACNiO-400-2, (f) ACNiO-500-2

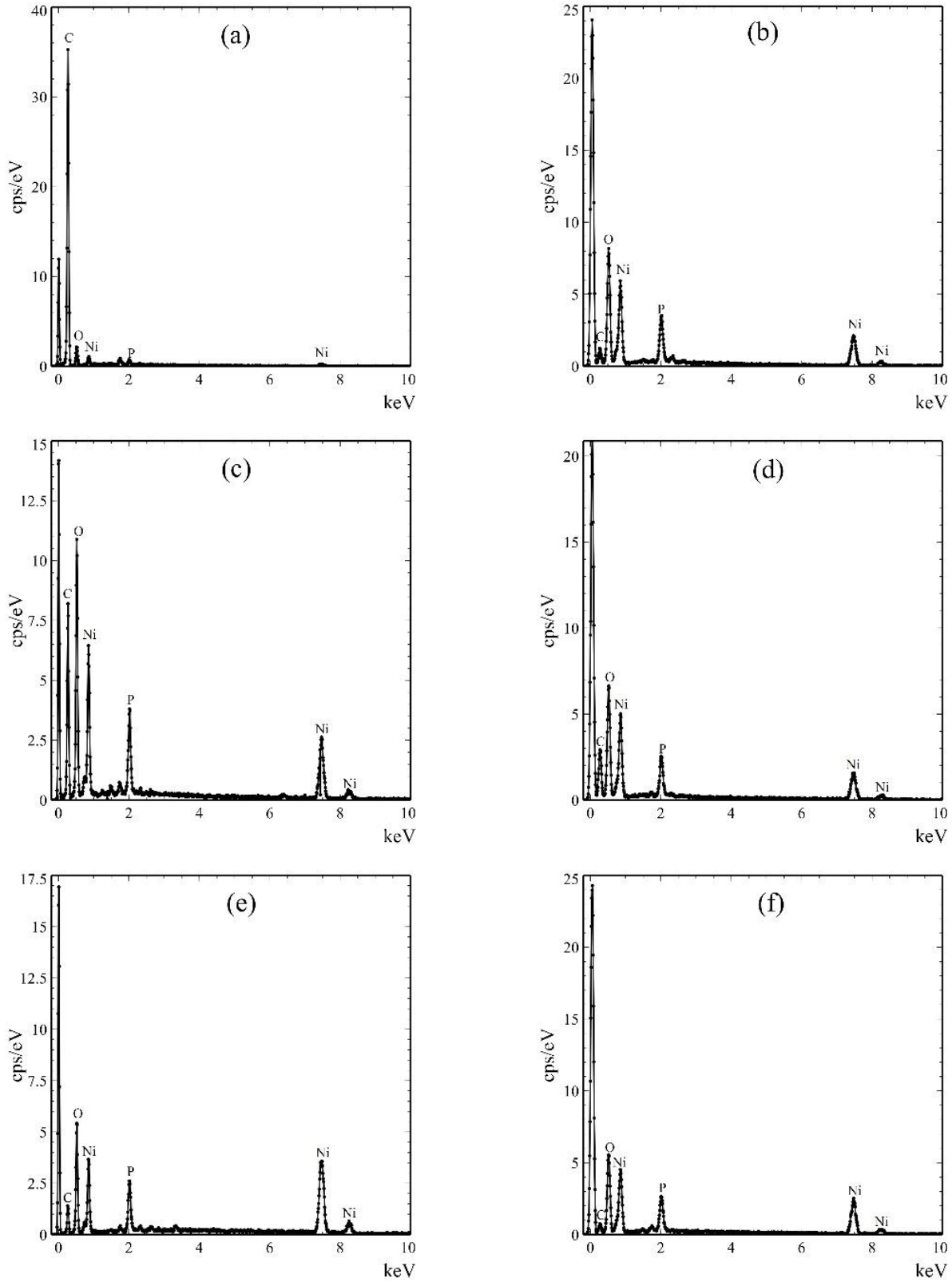

Figure 4 EDS spectra of the (a) ACNiO-300-1, (b) ACNiO-400-1, (c) ACNiO-500-1, (d) ACNiO-300-2, (e) ACNiO-400-2, (f) ACNiO-500-2

Table 3 Composition of elements on the surface of the AC-NiO samples

Sample	Elemental composition (wt %)			
	Ni	C	O	P
(a) ACNiO-300-1	4.2	82.2	12.6	0.9
(b) ACNiO-400-1	46.6	30.2	14.7	8.5
(c) ACNiO-500-1	36.2	36.0	23.3	4.5
(d) ACNiO-300-2	34.3	14.7	30.2	5.7
(e) ACNiO-400-2	70.6	11.8	12.5	5.0
(f) ACNiO-500-2	58.9	10.6	23.0	7.5

3.4 Crystalline-phase Analysis of AC-NiO Nanocomposites

Figure 5 shows the XRD patterns of the AC-NiO nanocomposite samples heated at various temperatures and time. From the figure, it can be observed that the samples calcinated at 300 and 400 °C for 1 h and the sample calcinated at 300 °C for 2 h show no diffraction peak due to nickel oxide loading just like the activated carbon substrate. Thus indicating that the nickel oxide was in an amorphous state. On the other hand, the sample treated at 500 °C for 1 h and the samples calcinated at 400 and 500 °C for 2 h, all clearly show the diffraction peaks at 2θ = 37.3°, 43.3°, 62.9°, 75.4° and 79.4° corresponding to (111), (200), (220), (311), and (222), respectively. All the identified peaks can be assigned to the cubic phase of NiO (JCPDS card no 00-004-0835). Also, the results show that the samples are phase-pure of NiO with no impurity peaks. The results are similar to the result obtained by Wang et al. [5]. Furthermore, the results show that the intensity increases with increasing in the calcination temperature and time, signifying that better crystallinity of NiO are formed at a higher temperature. This can be attributed to the decreasing carbon content. High carbon content suppresses crystallite growth [10].

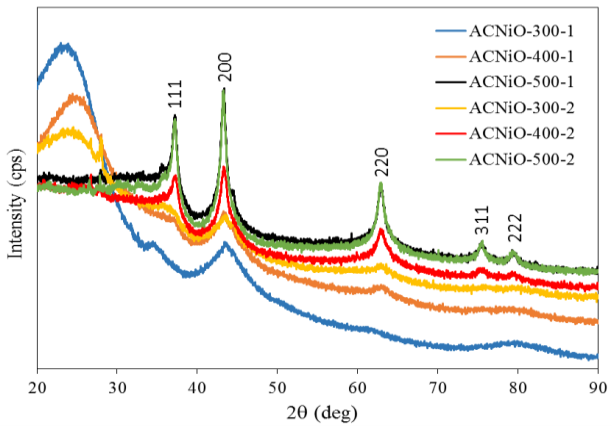

Figure 5 XRD patterns of AC-NiO nanocomposite samples

3.5 Effect of Heat Treatment Conditions on the BET Surface Area of the AC-NiO Samples

The BET surface area of the AC-NiO samples is presented in Table 4. According to the data in Table 4, the BET surface area of the samples decreases with the increase in the calcination temperature and time with respect to the BET surface area of the as-prepared activated carbon (OPSAC). At low temperature of 300 °C and time 1 h, the effect is not significant, but as the calcination temperature and time increase, there is progressive widening and merging of pores resulting in the development of more mesopores and attendant lower BET surface area.

Table 4 BET surface area of the AC-NiO samples

Sample	BET surface area (m^2/g)
(a) ACNiO-300-1	570.56
(b) ACNiO-400-1	326.26
(c) ACNiO-500-1	46.27
(d) ACNiO-300-2	380.96
(e) ACNiO-400-2	138.50
(f) ACNiO-500-2	27.39

4.0 CONCLUSION

Heat treatment usually carried out to accomplish the electroless deposition has been found to have a significant effect on the structure of the deposit. It has been observed that the flaky morphology structure of the composite grows rapidly with an increase in the heat treatment temperature. The weight percent composition of the nickel was found to increase with increasing of the treatment time.

Acknowledgement

The authors are appreciative of the Research University Grant Vot No 10H23 and 4L600 provided in part by the Ministry of Higher Education, Malaysia and UTM used to fund the research activity. Also, the authors wish to acknowledge Abubakar Tafawa Balewa University, Bauchi and TetFund Nigeria for the intervention program.

References

[1] Jia, B., Su, L., Han, G., Wang, G., Zhang, J., and Wang, L. 2011. Adsorption Properties of Nickel-Based Magnetic Activated Carbon Prepared by Pd-Free Electroless Plating. *BioResources*. 6(1): 70-80.

[2] Hsieh, C.-T. and Lin, J.-Y. 2009. Fabrication of Bimetallic Pt–M (M = Fe, Co, and Ni) Nanoparticle/carbon Nanotube Electrocatalysts for Direct Methanol Fuel Cells. *Journal of Power Sources*. 188(2): 347-352.

[3] Figueroa-Torres, M. Z., Domínguez-Ríos, C., Cabañas-Moreno, J. G., Vega-Becerra, O., and Aguilar-Elguézabal, A. 2012. The Synthesis of Ni-activated Carbon Nanocomposites Via Electroless Deposition without a Surface Pretreatment as Potential Hydrogen Storage Materials. *International Journal of Hydrogen Energy*. 37(14): 10743-10749.

[4] Liu, Y., Teng, H., Hou, H., and You, T. 2009. Nonenzymatic Glucose Sensor Based on Renewable Electrospun Ni Nanoparticle-loaded Carbon Nanofiber Paste Electrode. *Biosensors and Bioelectronics*. 24(11): 3329-3334.

[5] Wang, K., Li, L., and Zhang, H. 2013. Synthesis of Nickel Oxide/Active Carbon and Electrochemical Performance. *Int. J. Electrochem. Sci.* 8: 5036-5041.

[6] Faraji, S. and Ani, F. N. 2014. Microwave-assisted Synthesis of Metal Oxide/Hydroxide Composite Electrodes for High Power Supercapacitors – A Review. *Journal of Power Sources*. 263: 338-360.

[7] Zubizarreta, L., Menéndez, J. A., Pis, J. J., and Arenillas, A. 2009. Improving Hydrogen Storage in Ni-doped Carbon Nanospheres. *International Journal of Hydrogen Energy*. 34(7): 3070-3076.

[8] Jin, G.-P., Ding, Y.-F., and Zheng, P.-P. 2007. Electrodeposition of Nickel Nanoparticles on Functional MWCNT surfaces for Ethanol Oxidation. *Journal of Power Sources*. 166(1): 80-86.

[9] Aravinda, L. S., Nagaraja, K. K., Bhat, K. U., and Bhat, B. R. 2013. Magnetron Sputtered MoO_3/carbon Nanotube Composite Electrodes for Electrochemical Supercapacitor. *Journal of Electroanalytical Chemistry*. 699: 28-32.

[10] Chang, S.-K., Zainal, Z., Tan, K.-B., Yusof, N. A., Yusoff, W. M. D. W., and Prabaharan, S. R. S. 2012. Nickel–cobalt Oxide/activated Carbon Composite Electrodes for Electrochemical Capacitors. *Current Applied Physics*. 12(6): 1421-1428.

[11] Mallory, G. O. and Hajdu, J. B., eds. *Electroless Plating - Fundamentals & Applications*. 1990. American Electroplaters and Surface Finishers Society: Orlando, Florida. 532.

[12] Faraji, S. and Ani, F. N. 2015. The Development Supercapacitor from Activated Carbon by Electroless Plating—A Review. *Renewable and Sustainable Energy Reviews*. 42(0): 823-834.

[13] Brenner, A. and Riddell, G. E. 1946. Nickel Plating on Steel by Chemical Reduction. *Journal of Research of the National Bureau of Standards*. 37(31): 31-34.

[14] Brenner, A. and Riddell, G. E. 1950. Nickel Plating by Chemical Reduction. USpatent 2 532 283. Dec. 5, 1950.

[15] Ashassi-Sorkhabi, H. and Rafizadeh, S. H. 2004. Effect of Coating Time and Heat Treatment on Structures and Corrosion Characteristics of Electroless Ni–P alloy Deposits. *Surface and Coatings Technology*. 176(3): 318-326.

[16] Singh, D., Balasubramaniam, R., and Dube, R. K. 1995. Effect of Coating Time on Corrosion Behavior of Electroless Nickel-Phosphorus Coated Powder Metallurgy Iron Specimens. *Corrosion*. 51(8): 581-585.

[17] Ramani, M., Haran, B. S., White, R. E., Popov, B. N., and Arsov, L. 2001. Studies on Activated Carbon Capacitor Materials Loaded with Different Amounts of Ruthenium Oxide. *Journal of Power Sources*. 93(1-2): 209-214.

[18] Hu, Q.-h., Wang, X.-t., Chen, H., and Wang, Z.-f. 2012. Synthesis of Ni/graphene Sheets by an Electroless Ni-Plating Method. *New Carbon Materials*. 27(1): 35-41.

[19] Atieh, M. A., Bakather, O. Y., Al-Tawbini, B., Bukhari, A. A., Abuilaiwi, F. A., and Fettouhi, M. B. 2010. Effect of Carboxylic Functional Group Functionalized on Carbon Nanotubes Surface on the Removal of Lead from Water. *Bioinorganic Chemistry and Applications*. 2010: 603978.

[20] Deng, H., Yang, L., Tao, G., and Dai, J. 2009. Preparation and Characterization of Activated Carbon from Cotton Stalk by Microwave Assisted Chemical Activation--Application In Methylene Blue Adsorption from Aqueous Solution. *J Hazard Mater*. 166(2-3): 1514-21.

[21] Jahromi, S. P., Pandikumar, A., Goh, B. T., Lim, Y. S., Basirun, W. J., Lim, H. N., and Huang, N. M. 2015. Influence of particle Size on Performance of a Nickel Oxide Nanoparticle-Based Supercapacitor. *RSC Adv*. 5(18): 14010-14019.

[22] Sahoo, P. and Das, S. K. 2011. Tribology of Electroless Nickel Coatings – A Review. *Materials & Design*. 32(4): 1760-1775.